

Exact Solutions and Flow–Density Relations for a Cellular Automaton Variant of the Optimal Velocity Model with the Slow-to-Start Effect*

Hideaki Ujino[†]

*Gunma National College of Technology,
580 Toriba, Maebashi, Gunma 371–8530, Japan*

Tetsu Yajima[‡]

*Department of Information Science,
Graduate School of Engineering, Utsunomiya University,
7–1–2 Yoto, Utsunomiya, Tochigi 321–8585, Japan*

Abstract

A set of exact solutions for a cellular automaton, which is a hybrid of the optimal velocity and the slow-to-start models, is presented. The solutions allow coexistence of free flows and jamming or slow clusters, which is observed in asymptotic behaviors of numerically obtained spatio-temporal patterns. An exact expression of the flow–density relation given by the exact solutions of the model agrees with an empirical formula for numerically obtained flow–density relations.

Keywords: optimal velocity (OV) model, slow-to-start (s2s) effect, cellular automaton (CA), ultradiscretization, flow–density relation, exact solution

* Accepted for publication in J. Phys. Soc. Jpn.

[†] ujino@nat.gunma-ct.ac.jp

[‡] yajimat@is.utsunomiya-u.ac.jp

I. INTRODUCTION

Studies on microscopic models for vehicle traffic provided a good point of view on the phase transition from the free traffic flow to the congested one. Related self-driven many-particle systems have attracted considerable interests not only from engineers but also from physicists [1, 2]. Among such models, the optimal velocity (OV) model [3], which is a car-following model describing an adaptation to the optimal velocity that depends on the headway between two neighboring vehicles, is well-known for its successful rationalization of “phantom traffic jams” in the high-density regime.

Whereas the OV model consists of ordinary differential equations (ODE), cellular automata (CA) such as the Nagel–Schreckenberg model [4], the elementary CA of Rule 184 (ECA184) [5], the Fukui–Ishibashi (FI) model [6] and the slow-to-start (s2s) model [7] are extensively used in analyses of traffic flow. A way toward amalgamation of the ODE-type and the CA-type models was opened by the discovery of the discrete OV (dOV) model [8] that provides an ultradiscretization [9] of the OV model. The resultant ultradiscrete OV (uOV) model includes both the ECA184 and the FI model as its special cases. We should note here that another ultradiscretization [10] of the OV model is developed out of the ultradiscretization of the mKdV equation [11], which also has an application to the traffic flow [12].

Inspiration brought by the ultradiscretization of the OV model in ref. [8] leads us to an ultradiscretizable hybrid of the OV and the s2s models, which was named the optimal velocity model with the slow-to-start effect, or shortly, the s2s–OV model [13],

$$\frac{x_k(t)}{t} = v_0 \left(1 + \frac{1}{t_0} \int_0^{t_0} e^{-(\Delta x_k(t-t') - x_0)/\delta x} dt' \right)^{-1} - v_0 (1 + e^{x_0/\delta x})^{-1}, \quad (1)$$

where t_0 and $x_k(t)$ are the monitoring period and the position of the k -th car at the time t , respectively. The interval between the cars k and $k+1$ is denoted by $\Delta x_k(t) = x_{k+1}(t) - x_k(t)$. Sensitivity to the interval is controlled by $\delta x > 0$ and x_0 means the length of the road occupied by a vehicle. In the limit $t_0 \rightarrow 0$, the s2s–OV model reduces to the Newell model [14], which is a car-following model describing an retarded adaptation to the optimal velocity determined by the headway in the past. The ultradiscrete limit of the s2s–OV model includes a traffic-flow model of the CA-type,

$$x_k^{n+1} = x_k^n + \min \left(\min_{n'=0}^{n_0} (\tilde{\Delta} x_k^{n-n'}), v_0 \delta t \right), \quad (2)$$

where the position of the k -th car x_k^n , $k = 1, 2, \dots, K$, and the headway between the cars k and $k + 1$ at the n -th discrete time $\tilde{\Delta}x_k^n := x_{k+1}^n - x_k^n - x_0 \geq 0$ are integers. We should note that the headway $\tilde{\Delta}x_k^n$ and the interval $\Delta x_k^n := x_{k+1}^n - x_k^n = \tilde{\Delta}x_k^n + x_0$ between the cars k and $k + 1$ are used in different meanings in this paper. If all the initial headways $\tilde{\Delta}x_k^0$ are non-negative, then car crash is prohibited at any time. Positive integers v_0 , x_0 and δt means the speed limit, the size of a cell and the discrete time step, respectively. When we consider the time-evolution of the vehicles in the following, the latter two parameters, x_0 and δt , are fixed at one. Then eq. (2) reduces to

$$x_k^{n+1} = x_k^n + \min\left(\min_{n'=0}^{n_0}(x_{k+1}^{n-n'} - x_k^{n-n'} - 1), v_0\right). \quad (3)$$

We call a positive integer n_0 the monitoring period since the minimum of the headway $\tilde{\Delta}x_k^{n-n'} := x_{k+1}^{n-n'} - x_k^{n-n'} - x_0$ of $n_0 + 1$ discrete times, $n - n' = n - n_0, n - n_0 + 1, \dots, n$, is involved in the time evolution (2). This CA describes many cars running on a single lane highway in one direction, which is driven by cautious drivers requiring enough headway to go on at least for n_0 time steps before they accelerate their cars. Since the above CA (2) is an extension of the CA case of the uOV model [8] incorporating the s2s effect in the sense of delay in drivers' response, we call the CA (2) the CA variant of the OV model with the s2s effect, or the s2s-OVCA for short.

Figure 1 gives typical examples of the spatio-temporal pattern showing jams and the fundamental diagram of the s2s-OVCA [13]. The spatio-temporal pattern shows the trajectories of vehicles. Though irregular patterns are observed at the initial stage of time evolution, trajectories become regular in the long run, which consist of several jam clusters moving backward at the same velocity and vehicles running at the top speed. The fundamental diagram, or the flow-density relation, in other words, gives the relation between the vehicle flow

$$Q := \frac{1}{(n_f - n_i + 1)L} \sum_{k=1}^K \sum_{n=n_i}^{n_f} \frac{x_k^{n+1} - x_k^n}{\delta t},$$

which is equivalent to the total momentum of vehicles per unit length averaged over the period $n_i \leq n \leq n_f$ when the traffic is expected to be in equilibrium, and the vehicle density $\rho := \frac{K}{Lx_0}$ where L is the total number of the cells, or the length of the circuit, on which the periodic boundary condition is imposed. The fundamental diagram has the inverse- λ shape with several phases of traffic, namely, free, jam as well as metastable slow traffics, which captures the characteristic of observed flow-density relations [1, 2]. A comment here might

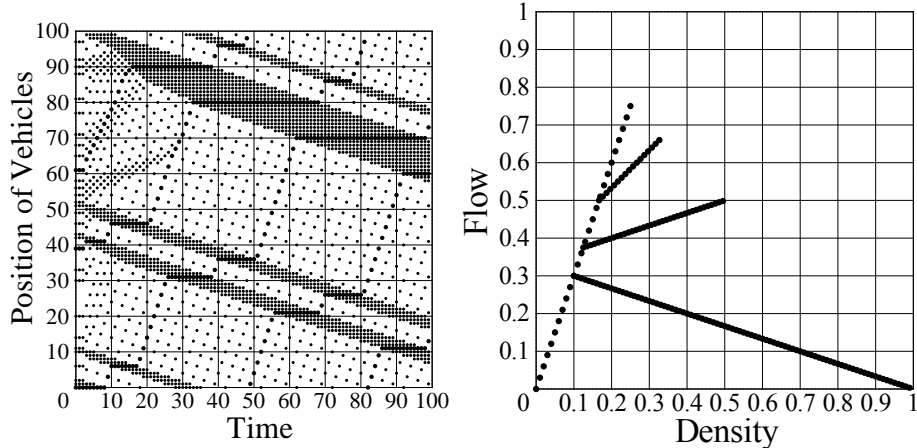


FIG. 1. The spatio-temporal pattern (left) and the fundamental diagram (right) of the s2s-OVCA [13]. The number of the cells L is fixed at $L = 100$ and the periodic boundary condition is imposed. The number of the cars in the above spatio-temporal pattern is $K = 30$. The maximum velocity v_0 and the monitoring period n_0 are $v_0 = 3$ and $n_0 = 2$. The flows Q are computed by averaging over the time period $800 \leq n \leq 1000$, in which the traffic is expected to be in equilibrium.

be in order. A CA-type model that is different from the s2s-OVCA showing a fundamental diagram with several branches was reported. [15] But all of its branches except for the free line have negative inclinations. This feature is also different from that of the fundamental diagram of the s2s-OVCA. As we can see in Fig. 1, the fundamental diagram consists of straight branches, whose number, four in this case, is the same as that of all possible integral velocities, $v = 0, 1, 2$ and $3(= v_0)$. The main result of this paper is to present a set of exact solutions of the s2s-OVCA, which explains the piecewise linear fundamental diagram of the s2s-OVCA.

The outline is as follows. In §II, the fundamental diagram given in Fig. 1 will be examined. An empirical formula for the fundamental diagram of the s2s-OVCA will be introduced. A set of exact solutions of the s2s-OVCA that reproduces the empirical formula will be presented in §III and §IV. Concluding remarks are given in the final section. Derivation of the s2s-OVCA (2) from the s2s-OV model (1) is briefly summarized in an appendix.

II. NUMERICAL OBSERVATION OF THE FUNDAMENTAL DIAGRAM

By numerical experiments [13], the fundamental diagram of the s2s–OVCA was observed to be piecewise linear and possesses v_0 branches irrespective of the parameter n_0 . Let us have a close look at the fundamental diagram in Figs. 1 and II and examine these features more in detail.

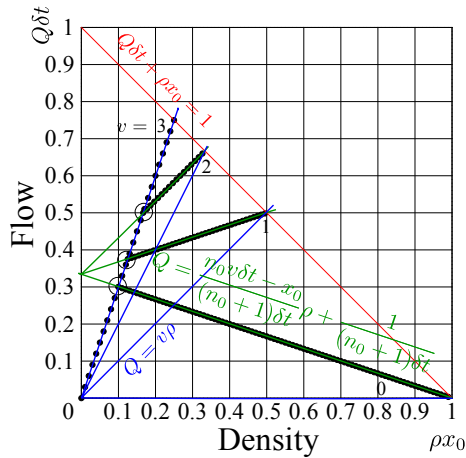


FIG. 2. (Color online) An empirical formula for the fundamental diagram of the s2s–OVCA. All the dots on the diagram were numerically computed [13] for the case in which the maximum velocity v_0 and the monitoring period n_0 are $v_0 = 3$ and $n_0 = 2$. Each solid line corresponds to the formula in the same color or in the same grayscale. Each branch is labeled with a number that shows the integral velocity v corresponding to the branch. The end points of the branches are determined by the maximum density for each integral velocity. The branch points of the slow or the jamming lines, which are encircled with thin small circles, give the lowest densities for these lines.

As shown in Fig. II, each branch corresponds to an integral velocity that is less than or equal to the maximum velocity v_0 . All the end points of the branches are observed to be on the line

$$Q\delta t + \rho x_0 = 1. \quad (4)$$

This is because the density at the end point is determined by the maximum density $\rho_{\max}(v)$ that allows the velocity of the slowest car to be v . Because of the time evolution of the s2s–OVCA (2), a car running at a velocity v must have an interval that is larger than or equal to $v\delta t + x_0$. Imagining a traffic such that all the cars flow at the same velocity v with

the minimum interval $v\delta t + x_0$, we conclude that the maximum density $\rho_{\max}(v)$ is determined by

$$\rho_{\max}(v) = \frac{1}{v\delta t + x_0}, \quad (5)$$

since each car occupies $v\delta t + x_0$ cells. The flow corresponding to the traffic is given by

$$Q(\rho_{\max}(v)) = v\rho_{\max}(v). \quad (6)$$

Equations (5) and (6) simultaneously holds on the end points and they yield $Q(\rho_{\max}(v))\delta t + \rho_{\max}(v)x_0 = 1$. Thus all the end points must satisfy the relation (4).

The free line is a branch that agrees with the straight line whose inclination equals to the maximum velocity v_0 ,

$$Q = v_0\rho, \quad (7)$$

since all the cars on the free line flow at the maximum speed v_0 . Any other branches branch off from the free line. By observation, the density of the branching point of the branch corresponding to a velocity v reads

$$\rho_{\min}(v) = \frac{1}{n_0(v_0 - v)\delta t + v_0\delta t + x_0}. \quad (8)$$

This observation is explained as follows. Suppose one car, say the car k , runs at the velocity v and all the other $K - 1$ cars run at the maximum velocity v_0 . At the moment the k -th car slows down to v , the interval between the cars k and $k + 1$ is $v\delta t + x_0$. Since it takes at least $n_0 + 1$ time steps for the car k to speed up to v_0 , the interval between the cars k and $k + 1$ expands up to $H = (n_0 + 1)(v_0 - v)\delta t + v\delta t + x_0 = 1/\rho_{\min}(v) > v_0\delta t$ by the time the k -th car speeds up to v_0 . If all the cars can obtain the interval H , slow cars running at the velocity v should vanish in the end. Thus the density at the branching point of the branch corresponding to the velocity $v\delta t$ is given by $\rho_{\min}(v) = 1/H$, which is nothing but the minimum density of the branch.

Suppose the slow branches form straight lines. Then these lines must be the segments connecting the branching point $(\rho_{\min}(v), v_0\rho_{\min}(v))$ and the end point $(\rho_{\max}(v), v\rho_{\max}(v))$. The expression for these line segments is obtained by eqs. (5), (6) and (8) as

$$Q = \frac{n_0v\delta t - x_0}{(n_0 + 1)\delta t}\rho + \frac{1}{(n_0 + 1)\delta t}, \quad (9)$$

which agrees fairly well with the branches for the slow traffics consisting of the numerically obtained dots in Fig. II. Coincidence of the Q -interception of slow branches $\frac{1}{(n_0+1)\delta t}$, which also appears in Fig. II, is also shown in the above empirical formula.

The aim of the following two sections is to explain the empirical formula for the fundamental diagram (9) based on exact solutions of the s2s-OVCA.

III. SOLUTIONS WITH A SINGLE SLOW CLUSTER

After transient flow goes on evolving irregularly for a while, the traffic reaches “equilibrium” in the long run where slow-traffic clusters of seemingly invariant sizes move regularly, as one can see in the spatio-temporal pattern in Fig. 1. Here we allow equilibrium to change sizes of slow or fast clusters periodically but prohibit it from increasing or decreasing their sizes monotonically. We shall investigate such equilibrium flows and their flow–density relations. Limiting ourselves to simple cases, we begin with equilibrium flows with, at most, a single slow cluster.

To begin with, we shall see a specific spatio-temporal pattern starting from the following initial configuration,

$$0 : 1\sqcup 2\sqcup 3\sqcup 4\sqcup\sqcup\sqcup\sqcup\sqcup\sqcup\sqcup\sqcup\sqcup 5\sqcup\sqcup\sqcup\sqcup. \quad (10)$$

Note that the number 0 at the leftmost shows the time. The digits and the blank symbols \sqcup in the above configuration mean the indices of the cars and the empty cells, respectively. We set the monitoring period n_0 at 2. The velocity of the cars 4 and 5 is 3, which is the top velocity v_0 of this case. The velocity of the cars 1, 2 and 3, whose headways are 1, is 1. Then in this case, the headways of all the cars in the past have nothing to do with the time evolution starting from the above configuration (10). The periodic boundary condition is assumed so the length of the circuit is 19 in this case.

Using eq. (3), which is equivalent to the s2s-OVCA (2) with $x_0 = \delta t = 1$, we can confirm that the following spatio-temporal pattern evolves out of the above initial configuration (10),

$$\begin{aligned} 0 & : 1\sqcup 2\sqcup 3\sqcup 4\sqcup\sqcup\sqcup\sqcup\sqcup\sqcup\sqcup\sqcup\sqcup 5\sqcup\sqcup\sqcup\sqcup \\ 1 & : \sqcup 1\sqcup 2\sqcup 3\sqcup\sqcup\sqcup 4\sqcup\sqcup\sqcup\sqcup\sqcup\sqcup\sqcup 5\sqcup \\ 2 & : 5\sqcup 1\sqcup 2\sqcup 3\sqcup\sqcup\sqcup\sqcup 4\sqcup\sqcup\sqcup\sqcup\sqcup \\ 3 & : \sqcup 5\sqcup 1\sqcup 2\sqcup 3\sqcup\sqcup\sqcup\sqcup\sqcup\sqcup 4\sqcup\sqcup\sqcup. \end{aligned} \quad (11)$$

Moving all the cells of the initial configuration one cell rightward as well as neglecting the difference of the car indices, we get the configuration at the time 3. In this sense, the initial configuration (10) gives a periodic motion of the vehicles and hence an equilibrium flow of

The circuit length L , which is shown under the brace in the above configuration, is then given by

$$L = L_0 - (n_0 - m)(v_0 - v)\delta t - lx_0, \quad (13)$$

where $L_0 := (K - k)(n_0 + 1)(v_0 - v)\delta t + K(x_0 + v\delta t)$. With use of $\rho_{\min}(v)$ given in eq. (8), the formula for the circuit length (13) is cast into

$$k(n_0 + 1)(v_0 - v)\delta t = \frac{K}{\rho_{\min}(v)} - L - (n_0 - m)(v_0 - v)\delta t - lx_0, \quad (14)$$

where $1/\rho_{\min}(v)$ is an integer. Since the parameter k gives the number of cars in a slow cluster, it must be non-negative. Equation (14) gives the condition for k to be non-negative as

$$0 \leq \frac{K}{\rho_{\min}(v)} - L - (n_0 - m)(v_0 - v)\delta t - lx_0.$$

Thus we obtain the necessary condition for k to be non-negative as

$$\rho := \frac{K}{L} \geq \rho_{\min}(v), \quad (15)$$

since $\frac{(n_0 - m)(v_0 - v)\delta t + lx_0}{L} \geq 0$. The lower bound of ρ in the above inequality coincides with the numerically obtained minimum density (8) for the branch corresponding to a velocity v .

We should confirm here that there always exist non-negative integers k, l and m satisfying eq. (13) for arbitrarily given L, K, n_0, v_0 and v that meet the condition (15). The r.h.s. of eq. (14) must be divided by $(n_0 + 1)(v_0 - v)\delta t$. Since the third and fourth terms cover all the residue classes modulo $(n_0 + 1)(v_0 - v)\delta t$, there always exist some non-negative integers k, l and m satisfying the above equation for arbitrary L, K, n_0, v_0 and v .

The time evolution out of the initial configuration (12) gives an equilibrium flow with a single slow cluster. Let us confirm it by checking each step of the time evolution. We exclude the case $k = K$ and shall deal with it separately. Watching the initial state again,

$$0 : | \langle v \rangle \xrightarrow{1} [0] \dots \langle v \rangle \xrightarrow{k-1} [0] \xrightarrow{k} \langle v \rangle \rightsquigarrow [0] \xrightarrow{k+1} [n_0+1] \dots \langle v_0 \rangle \xrightarrow{K-1} [n_0+1] \xrightarrow{K} \langle v_0 \rangle \rightsquigarrow [m+1]^{-lx_0}, \quad (16)$$

where 0 at the leftmost shows the time, we notice that the cars 1 to k run at a slow velocity v and the cars $k + 1$ to K run at the top velocity v_0 . Thus only two headways denoted by wavy arrows for clarity, namely those of the cars k and K that are the tops of the slow cluster and the fast cluster respectively, are going to change by $(v_0 - v)\delta t$ at each step. The configuration of the next time step is then given by

$$1 : | \xrightarrow{v\delta t} \langle v \rangle \xrightarrow{1} [0] \dots \langle v \rangle \xrightarrow{k-1} [0] \xrightarrow{k} \langle v \rangle \rightsquigarrow [1] \xrightarrow{k+1} [n_0+1] \dots \langle v_0 \rangle \xrightarrow{K-1} [n_0+1] \xrightarrow{K} \langle v_0 \rangle \rightsquigarrow [m]^{-lx_0}.$$

The subscript 1 of the car k shows that it is the first turn for the car k to have a headway which is long enough, $[1] = v_0\delta t$, to run at the top speed v_0 . Similarly, a subscript n of the k -th car, $\langle v \rangle_n^k$, $v < v_0$, whose headway is longer than or equal to $v_0\delta t$, means that it is the n -th turn for the car to have its headway long enough to run at the maximum velocity v_0 . This symbol is going to appear shortly and to be used in the same meaning in the following. The thick arrow at the leftmost shows the displacement of the car 1 from its initial cell. Until the car K decelerates at the m -th time step, the cars 1 to k run at a slow velocity v and all the others run at the top speed v_0 . Thus the configuration at the n -th time step, $1 \leq n \leq m - 1$, is expressed by

$$n : | \xRightarrow{nv\delta t} \langle v \rangle \xrightarrow{[0]} \dots \langle v \rangle \xrightarrow{[0]} \langle v \rangle_n^k \xrightarrow{[n]} \langle v_0 \rangle^{k+1} \xrightarrow{[n_0+1]} \dots \langle v_0 \rangle^{K-1} \xrightarrow{[n_0+1]} \langle v_0 \rangle^K \xrightarrow{[m+1-n]-lx_0} . \quad (17)$$

At the m -th time step, the headway of the car K shortens to $[1] - lx_0 = v_0\delta t - lx_0$ and its velocity immediately slows down to $v_0 - lx_0/\delta t$. Thus there additionally appears another varying headway denoted by a wavy arrow in front of the car $K - 1$. The configuration at the m -th time step is then given by

$$m : | \xRightarrow{mv\delta t} \langle v \rangle \xrightarrow{[0]} \dots \langle v \rangle \xrightarrow{[0]} \langle v \rangle_m^k \xrightarrow{[m]} \langle v_0 \rangle^{k+1} \xrightarrow{[n_0+1]} \dots \langle v_0 \rangle^{K-1} \xrightarrow{[n_0+1]} \langle v_0 - lx_0/\delta t \rangle^K \xrightarrow{[1]-lx_0} . \quad (18)$$

At this moment, velocities of the cars $K - 1$, K and 1 are respectively v_0 , $v_0 - lx_0/\delta t$ and v , as well as the headways of the cars $K - 1$ and K irregularly shortens by lx_0 and $(v_0 - v)\delta t - lx_0$. We classify the car K with the intermediate velocity $v_0 - lx_0/\delta t$ into the fast cluster. The slow cluster with the velocity v consists of cars with only a single slow velocity v . Thus the car K has been the top of the fast cluster by this turn. But in the next turn, the car K also slows down to v and becomes the bottom of the slow cluster. Thus the configuration at the $(m + 1)$ -th time step is

$$m + 1 : | \xRightarrow{(m+1)v\delta t} \langle v \rangle \xrightarrow{[0]} \dots \langle v \rangle \xrightarrow{[0]} \langle v \rangle_{m+1}^k \xrightarrow{[m+1]} \langle v_0 \rangle^{k+1} \xrightarrow{[n_0+1]} \dots \langle v_0 \rangle^{K-2} \xrightarrow{[n_0+1]} \langle v_0 \rangle^{K-1} \xrightarrow{[n_0+1]-lx_0} \langle v \rangle^K \xrightarrow{[0]} .$$

Until the car k accelerates at the $(n_0 + 1)$ -th time step, $k + 1$ cars, namely the cars 1 to k as well as the car K , run at a slow velocity v and all the others run at the top speed v_0 . Thus the configuration at the n -th time step, $m + 1 \leq n \leq n_0$, is expressed by

$$n : | \xRightarrow{nv\delta t} \langle v \rangle \xrightarrow{[0]} \dots \langle v \rangle \xrightarrow{[0]} \langle v \rangle_n^k \xrightarrow{[n]} \langle v_0 \rangle^{k+1} \xrightarrow{[n_0+1]} \dots \langle v_0 \rangle^{K-2} \xrightarrow{[n_0+1]} \langle v_0 \rangle^{K-1} \xrightarrow{[n_0-n+m+2]-lx_0} \langle v \rangle^K \xrightarrow{[0]} . \quad (19)$$

At the $(n_0 + 1)$ -th time step, the car k accelerates to the top velocity v_0 since its headway has kept no less than $v_0\delta t$ for n_0 time steps by the time. Thus the car k switches to the fast

cluster and the cars 1 to $k - 1$ as well as the car K now form the slow cluster. The place of the varying headway denoted by a wavy arrow also moves from the car k to the car $k - 1$. Thus the configuration at the $(n_0 + 1)$ -th time step looks as

$$n_0 + 1 : | \overset{(n_0+1)v\delta t}{\Rightarrow} \langle v \rangle \xrightarrow{[0]} \dots \langle v \rangle \overset{k-1}{\rightsquigarrow} \langle v_0 \rangle \xrightarrow{[n_0+1]} \langle v_0 \rangle \xrightarrow{[n_0+1]} \dots \langle v_0 \rangle \xrightarrow{[n_0+1]} \langle v_0 \rangle \overset{K-1}{\rightsquigarrow} \langle v_0 \rangle \xrightarrow{[m+1]-lx_0} \langle v \rangle \xrightarrow{[0]} . \quad (20)$$

Since the vehicles are running on the circuit of the length L , we may put the car K behind the car 1. Then the configuration at the $(n_0 + 1)$ -th time step

$$n_0 + 1 : | \overset{n_0v\delta t-x_0}{\Rightarrow} \langle v \rangle \xrightarrow{[0]} \langle v \rangle \xrightarrow{[0]} \dots \langle v \rangle \overset{k-1}{\rightsquigarrow} \langle v_0 \rangle \xrightarrow{[n_0+1]} \dots \langle v_0 \rangle \xrightarrow{[n_0+1]} \langle v_0 \rangle \overset{K-1}{\rightsquigarrow} \langle v_0 \rangle \xrightarrow{[m+1]-lx_0} , \quad (21)$$

becomes the same as the initial configuration up to the rightward displacement of $n_0v\delta t - x_0$ cells. Thus the motion of vehicles evolving out of the initial configuration (16) is periodic with the period $n_0 + 1$, which shows the corresponding traffic is in equilibrium.

The configuration for the case $k = K$

$$n : | \overset{nv\delta t}{\Rightarrow} \langle v \rangle \xrightarrow{[0]} \dots \langle v \rangle \xrightarrow{[0]}$$

gives a constant traffic flow in which all the cars run at the slow velocity v with the same headway $[0] = v\delta t$. Thus we confirm that the case $k = K$ also gives an equilibrium traffic.

We should note that the fast cluster in the case $k = K - 1$ temporally vanishes from the $(m + 1)$ -th time step to the n_0 -th time step,

$$\begin{aligned} 0 : & | \langle v \rangle \xrightarrow{[0]} \dots \langle v \rangle \xrightarrow{[0]} \langle v \rangle \overset{K-1}{\rightsquigarrow} \langle v_0 \rangle \xrightarrow{[m+1]-lx_0} , \\ n : & | \overset{nv\delta t}{\Rightarrow} \langle v \rangle \xrightarrow{[0]} \dots \langle v \rangle \xrightarrow{[0]} \langle v \rangle \overset{n}{\rightsquigarrow} \langle v_0 \rangle \xrightarrow{[m+1-n]-lx_0} , \quad 1 \leq n \leq m - 1, \\ m : & | \overset{mv\delta t}{\Rightarrow} \langle v \rangle \xrightarrow{[0]} \dots \langle v \rangle \xrightarrow{[0]} \langle v \rangle \overset{m}{\rightsquigarrow} \langle v_0 - lx_0/\delta t \rangle \xrightarrow{[1]-lx_0} , \\ n : & | \overset{nv\delta t}{\Rightarrow} \langle v \rangle \xrightarrow{[0]} \dots \langle v \rangle \xrightarrow{[0]} \langle v \rangle \overset{n}{\rightsquigarrow} \langle v_0 \rangle \xrightarrow{[m+1]-lx_0} \langle v \rangle \xrightarrow{[0]} , \quad m + 1 \leq n \leq n_0. \end{aligned} \quad (22)$$

But it appears again at the $(n_0 + 1)$ -th time step

$$n_0 + 1 : | \overset{(n_0+1)v\delta t}{\Rightarrow} \langle v \rangle \xrightarrow{[0]} \dots \langle v \rangle \xrightarrow{[0]} \langle v \rangle \overset{K-1}{\rightsquigarrow} \langle v_0 \rangle \xrightarrow{[m+1]-lx_0} \langle v \rangle \xrightarrow{[0]} ,$$

which goes back to the shifted initial configuration,

$$n_0 + 1 : | \overset{n_0v\delta t-x_0}{\Rightarrow} \langle v \rangle \xrightarrow{[0]} \langle v \rangle \xrightarrow{[0]} \dots \langle v \rangle \xrightarrow{[0]} \langle v \rangle \overset{K-1}{\rightsquigarrow} \langle v_0 \rangle \xrightarrow{[m+1]-lx_0} .$$

Thus such vanishment of the fast cluster as we have observed above does not break equilibrium of the traffic.

Now let us compute the flow of this periodic motion averaged over the period $n_0 + 1$. As we have already seen in the above time evolutions for the cases $k = 1, 2, \dots, K - 1$, k and $K - k$ cars respectively run at the velocities v and v_0 in $0 \leq n \leq m - 1$. At the m -th time step, k and $K - k - 1$ cars run at the velocities v and v_0 and remaining one car move at $v_0 - lx_0/\delta t$. In the following period, $m + 1 \leq n \leq n_0$, $k + 1$ and $K - k - 1$ cars move at the velocities v and v_0 , respectively. Thus the average flow Q is

$$\begin{aligned} Q &= \frac{1}{(n_0 + 1)L} \left(m(kv + (K - k)v_0) + (kv + (K - k - 1)v_0 + v_0 - lx_0/\delta t) \right. \\ &\quad \left. + (n_0 - m)((k + 1)v + (K - k - 1)v_0) \right) \\ &= \frac{n_0 v \delta t - x_0}{(n_0 + 1)\delta t} \rho + \frac{1}{(n_0 + 1)\delta t}, \end{aligned}$$

which is the same as the empirical formula for the flow–density relation (9). For the case $k = K$, the flow Q and the density ρ are respectively given by

$$Q = \rho v, \quad \rho = \frac{1}{v\delta t + x_0}.$$

A straightforward calculation shown below

$$\begin{aligned} Q &= \rho \frac{(n_0 + 1)v\delta t}{(n_0 + 1)\delta t} = \frac{(n_0 v \delta t - x_0) + (v\delta t + x_0)}{(n_0 + 1)\delta t} \rho \\ &= \frac{n_0 v \delta t - x_0}{(n_0 + 1)\delta t} \rho + \frac{1}{(n_0 + 1)\delta t} \end{aligned}$$

proves that the above two quantities are related by the flow–density relation (9).

The above formula is interpreted in a different and more intuitive manner. The configurations (16) and (21) shows the rightward displacement of the entire configuration (16) by $n_0 v \delta t - x_0$ cells in $n_0 + 1$ time steps. The flow provided by this motion of the entire configuration gives the first term $\frac{n_0 v \delta t - x_0}{(n_0 + 1)\delta t} \rho$ of the above formula. Here we should remind ourselves of the leftward displacement of the car K by L cells, namely whole the circuit length, which is fictitiously introduced to make the shifted initial configuration (21) from the real configuration (20) at the $(n_0 + 1)$ -th discrete time. In order to compensate the underestimation of the flow caused by this fictitious displacement, we have to add the flow corresponding to the rightward displacement of the car K by L cells in $n_0 + 1$ time steps

$$\frac{1}{(n_0 + 1)L} \cdot \frac{L}{\delta t} = \frac{1}{(n_0 + 1)\delta t},$$

which agrees with the second term of the above formula for the average flow.

IV. SOLUTIONS WITH MULTIPLE SLOW CLUSTERS

As we have observed in the spatio-temporal pattern in Fig. 1, several slow or jam clusters that share the same slow velocity coexist in equilibrium. Here we make solutions as such.

Roughly speaking, we can make an equilibrium solution with multiple slow clusters by putting several snapshots of the equilibrium solutions in the previous section together. Let us see how this idea works via observation of a specific example. Thanks to the periodic boundary condition, we can move the leftmost empty cell of the configuration (11) to the rightmost,

$$\begin{aligned} \sqcup 1 \sqcup 2 \sqcup 3 \sqcup \dots \sqcup 4 \sqcup \dots \sqcup 5 \sqcup &= | \xrightarrow{1} 1 \sqcup 2 \sqcup 3 \sqcup \dots \sqcup 4 \sqcup \dots \sqcup 5 \sqcup \\ &= | \xrightarrow{1} \langle 1 \rangle \xrightarrow{1} \langle 1 \rangle \xrightarrow{1} \langle 1 \rangle \xrightarrow{3} \langle 3 \rangle \xrightarrow{7} \langle 2 \rangle \xrightarrow{2} . \end{aligned}$$

Putting the above configuration and the configuration (10)

$$1 \sqcup 2 \sqcup 3 \sqcup 4 \sqcup \dots \sqcup 5 \sqcup \dots \sqcup = | \langle 1 \rangle \xrightarrow{1} \langle 1 \rangle \xrightarrow{1} \langle 1 \rangle \xrightarrow{3} \langle 3 \rangle \xrightarrow{7} \langle 3 \rangle \xrightarrow{4}$$

together, we get a configuration with two slow clusters as

$$\begin{aligned} 1 \sqcup 2 \sqcup 3 \sqcup \dots \sqcup 4 \sqcup \dots \sqcup 5 \sqcup 6 \sqcup 7 \sqcup 8 \sqcup 9 \sqcup \dots \sqcup 0 \sqcup \dots \sqcup \\ = \langle 1 \rangle \xrightarrow{1} \langle 1 \rangle \xrightarrow{1} \langle 1 \rangle \xrightarrow{3} \langle 3 \rangle \xrightarrow{7} \langle 2 \rangle \xrightarrow{2} \langle 1 \rangle \xrightarrow{1} \langle 1 \rangle \xrightarrow{1} \langle 1 \rangle \xrightarrow{3} \langle 3 \rangle \xrightarrow{7} \langle 3 \rangle \xrightarrow{4} \end{aligned} \quad (23)$$

Using eq. (3), we can confirm that the time evolution out of the above configuration gives a spatio-temporal patterns below,

$$\begin{aligned} 0 : & 1 \sqcup 2 \sqcup 3 \sqcup \dots \sqcup 4 \sqcup \dots \sqcup 5 \sqcup 6 \sqcup 7 \sqcup 8 \sqcup 9 \sqcup \dots \sqcup 0 \sqcup \dots \sqcup \\ 1 : & \sqcup 1 \sqcup 2 \sqcup 3 \sqcup \dots \sqcup 4 \sqcup \dots \sqcup 5 \sqcup 6 \sqcup 7 \sqcup 8 \sqcup \dots \sqcup 9 \sqcup \dots \sqcup 0 \sqcup \\ 2 : & 0 \sqcup 1 \sqcup 2 \sqcup 3 \sqcup \dots \sqcup 4 \sqcup \dots \sqcup 5 \sqcup 6 \sqcup 7 \sqcup 8 \sqcup \dots \sqcup 9 \sqcup \dots \sqcup \\ 3 : & \sqcup 0 \sqcup 1 \sqcup 2 \sqcup \dots \sqcup 3 \sqcup \dots \sqcup 4 \sqcup 5 \sqcup 6 \sqcup 7 \sqcup 8 \sqcup \dots \sqcup 9 \sqcup \dots \end{aligned}$$

Moving all the cells of the initial configuration one cell rightward as well as neglecting the difference of the car indices, we get the configuration at the time 3. Thus the configuration (23) gives a periodic motion of the vehicles and hence an equilibrium flow of the s2s-OVCA (2). In the following, we shall confirm that the above construction of equilibrium flows with multiple slow clusters works in general, too.

As building blocks of such solutions, we introduce symbols denoting slow and fast clusters in the snapshots of the equilibrium solutions (16), (17), (18) and (19) in the previous section,

$$n : | \xrightarrow{d} \langle S \rangle \xrightarrow{h_s} \langle F \rangle \xrightarrow{h_f}, \quad d = \begin{cases} nv\delta t & 0 \leq n \leq m \\ (n-1)v\delta t - x_0 & m+1 \leq n \leq n_0 \end{cases}, \quad (24)$$

where $\langle S \rangle \xrightarrow{h_s}$ and $\langle F \rangle \xrightarrow{h_f}$ respectively denote the slow and the fast clusters with varying headways $\xrightarrow{h_{s,f}}$ whose lengths are $h_{s,f}$ on their tops. For instance, the slow and fast clusters in the snapshot of the m -th time step (18) are respectively given by

$$\begin{aligned} \langle S \rangle \xrightarrow{h_s} & := \langle v \rangle \xrightarrow{[0]} \dots \langle v \rangle \xrightarrow{[0]} \langle v \rangle \xrightarrow{[m]} \\ \langle F \rangle_F \xrightarrow{h_f} & := \langle v_0 \rangle \xrightarrow{[n_0+1]} \dots \langle v_0 \rangle \xrightarrow{[n_0+1]} \langle v_0 - lx_0/\delta t \rangle \xrightarrow{[1]-lx_0}, \end{aligned}$$

where $h_s = [m]$ and $h_f = [1] - lx_0$. Note that the car K with the intermediate velocity $v_0 - lx_0/\delta t$ is classified into the fast cluster. We also note that we can always rearrange the order of the vehicles into the form of eq. (24), thanks to the periodic boundary condition.

An equilibrium solution with N slow clusters are made with the slow and fast clusters (24) with the same monitoring period n_0 , the slow velocity v and the top velocity v_0 . First, we prepare N pairs of slow and fast clusters in the configurations of N equilibrium solutions with only a single slow cluster, $\langle S_i \rangle \xrightarrow{h_{s_i}}, \langle F_i \rangle \xrightarrow{h_{f_i}}$ $i = 1, 2, \dots, N$. We shall consider a configuration made by putting these pairs of slow and fast clusters in line,

$$\langle S_1 \rangle \xrightarrow{h_{s_1}} \langle F_1 \rangle \xrightarrow{h_{f_1}} \langle S_2 \rangle \xrightarrow{h_{s_2}} \langle F_2 \rangle \xrightarrow{h_{f_2}} \dots \langle S_N \rangle \xrightarrow{h_{s_N}} \langle F_N \rangle \xrightarrow{h_{f_N}}. \quad (25)$$

where the periodic boundary condition is imposed. Thus the total length of the circuit is the sum of the lengths of all the clusters.

We observed that vanishment of a fast cluster (22) does not break equilibrium because the vanished fast cluster was revived by acceleration of the top car of the slow cluster behind. However, the top car of the fast cluster does not slow down if the slow cluster in front of it vanishes. Thus a vanishing slow cluster does break equilibrium. If slow down to the slow velocity v of the top car of any fast cluster $\langle F_i \rangle$ is no later than speed up to the top velocity v_0 of the bottom car of the slow cluster $\langle S_{i+1} \rangle$ in front of the fast cluster $\langle F_i \rangle$, such vanishment of slow clusters is prevented. Thus we require the above “no vanishing slow cluster” (NVSC) rule to be fulfilled by any pairs of the fast and slow clusters, $\langle F_i \rangle$ and $\langle S_{i+1} \rangle$, in the configurations (25).

We shall see below that the above configuration (25) satisfying the NVSC rule gives an equilibrium solution with N slow clusters. Speaking more specifically, we shall confirm that the motion of vehicles belonging to a pair of slow and fast clusters $\langle S_i \rangle \overset{h_{s_i}}{\rightsquigarrow} \langle F_i \rangle \overset{h_{f_i}}{\rightsquigarrow}$, $i = 1, 2, \dots, N$, in the above configuration (25) with multiple slow clusters is the same as that without any other pairs of slow and fast clusters we have investigated in detail in the previous section.

Consider the time evolution of a fast cluster and its varying headway $\langle F_i \rangle \overset{h_{f_i}}{\rightsquigarrow}$, $i = 1, 2, \dots, N$. It is determined by the motion of the vehicle at the bottom of the slow cluster $\langle S_{i+1} \rangle \overset{h_{s_{i+1}}}{\rightsquigarrow}$ in front of it, which is different from its original partner in the solution with a single slow-cluster $\langle S_i \rangle \overset{h_{s_i}}{\rightsquigarrow}$ behind it. However, thanks to the NVSC rule, the bottom of $\langle S_{i+1} \rangle \overset{h_{s_{i+1}}}{\rightsquigarrow}$ keeps the slow velocity v until the top of $\langle F_i \rangle \overset{h_{f_i}}{\rightsquigarrow}$ slows down to v . Thus the motion of the bottom of $\langle S_{i+1} \rangle \overset{h_{s_{i+1}}}{\rightsquigarrow}$ is the same as that of the bottom of $\langle S_i \rangle \overset{h_{s_i}}{\rightsquigarrow}$ and so is the motion of the fast cluster $\langle F_i \rangle \overset{h_{f_i}}{\rightsquigarrow}$ until its top slows down to v . Let us now think about the time evolution after the top of $\langle F_i \rangle \overset{h_{f_i}}{\rightsquigarrow}$ slows down to v . In the same manner we observed in the solution with only a single slow cluster in the previous section, the top of $\langle F_i \rangle \overset{h_{f_i}}{\rightsquigarrow}$ keeps the slow velocity v at least for $n_0 + 1$ time steps. The time evolution of the varying headway, which locates in front of the second car of $\langle F_i \rangle \overset{h_{f_i}}{\rightsquigarrow}$, and the motion of the remaining cars of $\langle F_i \rangle \overset{h_{f_i}}{\rightsquigarrow}$ are now determined by the above motion of the top of $\langle F_i \rangle \overset{h_{f_i}}{\rightsquigarrow}$. Thus the time evolution of the fast cluster and its varying headway $\langle F_i \rangle \overset{h_{f_i}}{\rightsquigarrow}$ remains the same as that with only a single slow cluster we observed in the previous section at least for $n_0 + 1$ time steps after the top of $\langle F_i \rangle \overset{h_{f_i}}{\rightsquigarrow}$ slows down to v and at least for $n_0 + 1$ time steps from the beginning.

Let us turn ourselves now to the time evolution of a slow cluster and its varying headway $\langle S_i \rangle \overset{h_{s_i}}{\rightsquigarrow}$, $i = 1, 2, \dots, N$. The time evolution is determined by the motion of the vehicle at the bottom of the fast cluster in front of it, which is nothing but its original partner in the solution with a single slow-cluster, $\langle F_i \rangle \overset{h_{f_i}}{\rightsquigarrow}$. We now know that the time evolution of the fast cluster $\langle F_i \rangle \overset{h_{f_i}}{\rightsquigarrow}$ is the same as those with only a single slow cluster for $n_0 + 1$ time steps. Thus the time evolution of the the slow cluster $\langle S_i \rangle \overset{h_{s_i}}{\rightsquigarrow}$ and its varying headway in the configuration with multiple slow clusters (25) is the same as that in the configuration with only a single slow cluster for $n_0 + 1$ time steps.

As we saw in the configuration with only a single slow cluster in the previous section, the time evolution of the slow and the fast clusters as well as their varying headways are periodic

with the period $n_0 + 1$. Thus, also in the configuration with multiple slow clusters (25), the time evolution of all of the slow and the fast clusters as well as their varying headways are periodic with the period $n_0 + 1$. To summarize, we have confirmed that the motion of vehicles belonging to a pair of slow and fast clusters $\langle S_i \rangle \overset{h_{s_i}}{\rightsquigarrow} \langle F_i \rangle \overset{h_{f_i}}{\rightsquigarrow}$, $i = 1, 2, \dots, N$, in the configuration (25) with multiple slow clusters is the same as that without any other pairs of slow and fast clusters we have investigated in detail in the previous section and that it gives an equilibrium solution with N slow clusters.

Let us examine the flow–density relation of the traffic evolving out of the configuration with N slow clusters (25). Let L_i , K_i , Q_i and $\rho_i := K_i/L_i$ be the circuit length, the number of vehicles, the mean flow averaged over one period, i.e. $n_0 + 1$ time steps, and the density of vehicles for the configuration with only one slow cluster, $\langle S_i \rangle \overset{h_{s_i}}{\rightsquigarrow} \langle F_i \rangle \overset{h_{f_i}}{\rightsquigarrow}$, $i = 1, 2, \dots, N$. In §III, we confirmed that Q_i and ρ_i satisfied the flow–density relation (9),

$$Q_i = \frac{n_0 v \delta t - x_0}{(n_0 + 1) \delta t} \rho_i + \frac{1}{(n_0 + 1) \delta t}. \quad (26)$$

The circuit length L and the number of vehicles K of the configuration with N slow clusters are then expressed by $L := \sum_{i=1}^N L_i$ and $K := \sum_{i=1}^N K_i$. The mean flow Q that is again averaged over the period as well as the vehicle density ρ of the configuration with N slow clusters are expressed by

$$Q = \frac{1}{L} \sum_{i=1}^N L_i Q_i = \sum_{i=1}^N \lambda_i Q_i,$$

$$\rho = \frac{K}{L} = \sum_{i=1}^N \lambda_i \rho_i,$$

with $\lambda_i := L_i/L$. Using an identity $\sum_{i=1}^N \lambda_i = 1$ as well as the flow density relation for the configuration with a single slow cluster (26), one straightforwardly confirms

$$\begin{aligned} Q - \frac{n_0 v \delta t - x_0}{(n_0 + 1) \delta t} \rho &= \sum_{i=1}^N \lambda_i \left(Q_i - \frac{n_0 v \delta t - x_0}{(n_0 + 1) \delta t} \rho_i \right) \\ &= \left(\sum_{i=1}^N \lambda_i \right) \frac{1}{(n_0 + 1) \delta t} = \frac{1}{(n_0 + 1) \delta t}, \end{aligned}$$

which concludes that Q and ρ also satisfy the flow–density relation (9). Note that the relation can be confirmed in a more intuitive manner, as we have shown for the configuration with only a single slow cluster.

V. CONCLUDING REMARKS

We have introduced a set of exact solutions of the s2s–OVCA and have explained the piecewise linear fundamental diagram of the model. The empirical formula for the flow–density relation of the s2s–OVCA (9) has been read out of the numerically obtained fundamental diagram in Figs. 1 and II. A set of exact periodic solutions that possesses only a single slow cluster has been presented, which has reproduced the formula for the flow–density relation of the s2s–OVCA (9). With the use of these solutions, another set of exact periodic solutions with multiple slow clusters, which have been observed in the numerically obtained spatio-temporal pattern in Fig. 1 has been introduced. And these solutions again have explained the flow–density relation of the s2s–OVCA (9).

We should comment about a couple of problems in our mind related to the present results. The solutions given in §III and §IV provide a set of equilibrium flows which correspond all the points on the fundamental diagram of the s2s–OVCA. But we do not know if the set we have presented in §III and §IV gives all possible equilibrium flows or not. There might be a solution giving an equilibrium flow that does not belong to the set. By numerical experiments [13], we observed that time evolutions out of all the initial conditions we verified eventually go to some equilibrium flows. But this observation still remains numerical observation and lacks proof. For the case of $n_0 = 1$, these problems were investigated [16] and should be extended to all the cases of n_0 's. As was shown in our previous paper [13], the s2s–OVCA (2) transforms to the s2s–OV model (1) through the inverse ultradiscretization and the continuous limit. Note that the monitoring period n_0 in the s2s–OVCA must be a free parameter so as to make the monitoring period t_0 in the s2s–OV model a free parameter. It should be clarified if the characteristics of the equilibrium solution of the s2s–OVCA given in this paper remain in the solution of the s2s–OV model.

ACKNOWLEDGMENTS

One of the authors (HU) is grateful to K. Oguma for the previous collaboration.

Appendix A

We shall derive the s2s–OVCA (2) from the s2s–OV model (1) in a brief way. Introducing the OV function

$$v_{\text{opt}}(x) := v_0 \left(\frac{1}{1 + e^{-(x-x_0)/\delta x}} - \frac{1}{1 + e^{x_0/\delta x}} \right)$$

as well as the effective distance

$$\Delta_{\text{eff}} x_k(t) := \delta x \log \left(\frac{1}{t_0} \int_0^{t_0} e^{-\Delta x_k(t-t')/\delta x} dt' \right)^{-1},$$

the s2s–OV model is expressed as

$$\frac{\dot{x}_k(t)}{t} = v_{\text{opt}}(\Delta_{\text{eff}} x_k(t)). \quad (\text{A1})$$

Let $x_k^n := x_k(t = n\delta t)$ and $v_k^n := (x_k^{n+1} - x_k^n)/\delta t$. Discretization of the effective distance $\Delta_{\text{eff}} x_k(t)$ is then expressed as

$$\Delta_{\text{eff}}^d x_k^n := \delta x \log \left(\sum_{n'=0}^{n_0} \frac{e^{-\Delta x_k^{n-n'}/\delta x}}{n_0 + 1} \right)^{-1},$$

where $n_0 := t_0/\delta t$. Using the fact that the OV function $v_{\text{opt}}(x)$ is written as a limit of a function

$$v_{\text{opt}}^d(x) := \frac{\delta x}{\delta t} \log \left[\frac{1 + e^{(x-x_0)/\delta x}}{1 + e^{-x_0/\delta x}} \bigg/ \frac{1 + e^{(x-x_0-v_0\delta t)/\delta x}}{1 + e^{-(x_0+v_0\delta t)/\delta x}} \right]$$

as $v_{\text{opt}}(x) = \lim_{\delta t \rightarrow 0} v_{\text{opt}}^d(x)$, the s2s–OV model (A1) in a time-discretized form is given by

$$v_k^n = v_{\text{opt}}^d(\Delta_{\text{eff}}^d x_k^n), \quad (\text{A2})$$

which is equivalent to

$$\begin{aligned} x_k^{n+1} = x_k^n + \delta x \left\{ \log \left[1 + \left(\sum_{n'=0}^{n_0} \frac{e^{-(\Delta x_k^{n-n'} - x_0)/\delta x}}{n_0 + 1} \right)^{-1} \right] - \log(1 + e^{-x_0/\delta x}) \right. \\ \left. - \log \left[1 + \left(\sum_{n'=0}^{n_0} \frac{e^{-(\Delta x_k^{n-n'} - x_0 - v_0\delta t)/\delta x}}{n_0 + 1} \right)^{-1} \right] + \log(1 + e^{-(x_0 + v_0\delta t)/\delta x}) \right\}. \end{aligned}$$

It is straightforward to confirm that the continuum limit $\delta t \rightarrow 0$ of the above discrete s2s–OV model (A2) reduces to eq. (A1) or equivalently the s2s–OV model (1).

Ultradiscretization [9] is a scheme for getting a piecewise-linear equation from a difference equation via the limit formula

$$\lim_{\delta x \rightarrow +0} \delta x \log(e^{A/\delta x} + e^{B/\delta x} + \dots) = \max(A, B, \dots).$$

In the ultradiscrete limit, the OV function for the discrete s2s–OV model $v_{\text{opt}}^{\text{d}}(x)$ goes to

$$\lim_{\delta x \rightarrow +0} v_{\text{opt}}^{\text{d}}(x) =: v_{\text{opt}}^{\text{u}}(x) = \max\left(0, \frac{x - x_0}{\delta t}\right) - \max\left(0, \frac{x - x_0}{\delta t} - v_0\right),$$

which is nothing but the OV function for the uOV model [8]. The effective distance $\Delta_{\text{eff}}^{\text{d}} x_k^n$ on the other hand is also ultradiscretized in the same manner:

$$\Delta_{\text{eff}}^{\text{u}} x_k^n := \lim_{\delta x \rightarrow +0} \Delta_{\text{eff}}^{\text{d}} x_k^n = -\max_{n'=0}^{n_0}(-\Delta x_k^{n-n'}) = \min_{n'=0}^{n_0}(\Delta x_k^{n-n'}).$$

Thus we obtain an ultradiscrete equation

$$v_k^n = v_{\text{opt}}^{\text{u}}(\Delta_{\text{eff}}^{\text{u}} x_k^n), \quad (\text{A3})$$

which is equivalent to

$$x_k^{n+1} = x_k^n + \max\left(0, \min_{n'=0}^{n_0}(\Delta x_k^{n-n'}) - x_0\right) - \max\left(0, \min_{n'=0}^{n_0}(\Delta x_k^{n-n'}) - x_0 - v_0 \delta t\right),$$

as the ultradiscrete limit of the discrete s2s–OV model (A2). We name it the ultradiscrete s2s–OV model.

Now let us see how the s2s–OVCA comes out from the ultradiscrete s2s–OV model (A3). Assume that the headway between the cars k and $k + 1$, $\tilde{\Delta} x_k^n := \Delta x_k^n - x_0$, for any k must be non-negative, $\tilde{\Delta} x_k^n \geq 0$, which prohibits car-crash from now on. Then the ultradiscrete s2s–OV model (A3) reduces to the s2s–OVCA (2). Note that the constants x_0 and $v_0 \delta t$ can be arbitrary in the above derivation. We set $x_0 = 1$ and $v_0 \delta t$ at an integer so that the positions of the vehicles x_k^n become integers at any time.

-
- [1] D. Chowdhury, L. Santen and A. Schadschneider: Phys. Rep. **329** (2000) 199.
 - [2] D. Helbing: Rev. Mod. Phys. **73** (2001) 1067.
 - [3] M. Bando, K. Hasebe, A. Nakayama, A. Shibata and Y. Sugiyama: Phys. Rev. E **51** (1995) 1035.
 - [4] K. Nagel and M. Schreckenberg: J. Physique I **2** (1992) 2221.
 - [5] S. Wolfram: *Theory and Applications of Cellular Automata* (World Scientific, Singapore, 1986).
 - [6] M. Fukui and Y. Ishibashi: J. Phys. Soc. Jpn. **65** (1996) 1868.

- [7] M. Takayasu and H. Takayasu: *Fractals* **1** (1993) 860.
- [8] D. Takahashi and J. Matsukidaira: *JSIAM Letters* **1** (2009) 1.
- [9] T. Tokihiro, D. Takahashi, J. Matsukidaira and J. Satsuma: *Phys. Rev. Lett.* **76** (1996) 3247.
- [10] M. Kanai, S. Isojima, K. Nishinari and T. Tokihiro: *Phys. Rev. E* **79** (2009) 056108.
- [11] D. Takahashi and J. Matsukidaira: *J. Phys. A: Math. Gen.* **30** (1997) L733.
- [12] H. Emmerich, T. Nagatani and K. Nakanishi: *Physica A* **254** (1998) 548.
- [13] K. Oguma and H. Ujino: *JSIAM Letters* **1** (2009) 68.
- [14] G. F. Newell: *Oper. Res.* **9** (1961) 209.
- [15] K. Nishinari, M. Fukui and A. Schadschneider: *J. Phys. A: Math. Gen.* **37** (2004) 3101.
- [16] R. Tian: *Disc. Appl. Math.* **157** (2009) 2904.